Stepan SAVCHUK
Polish Air Force University
e-mail: s.savchuk@law.mil.pl
ORCID: 0000-0002-2475-9666

Janusz ĆWIKLAK
Polish Air Force University
e-mail: j.cwiklak@law.mil.pl
ORCID: 0000-0001-5538-0440

Vladyslav KERKER
Lviv Polytechnic National University
e-mail: vladyslav.kerker.mhdkh.2022@lpnu.ua
ORCID: 00009-0007-3756-8125

DOI: 10.55676/asi.v3i1.54

ACCURACY ASSESSMENT OF PRECISE POINT POSITIONING WITH MULTI-CONSTELLATION GNSS DATA UNDER STRONG SOLAR BURST EFFECTS

OCENA DOKŁADNOŚCI PRECYZYJNEGO POZYCJONOWANIA PUNKTÓW NA PODSTAWIE DANYCH MULTI-GNSS PRZY SILNYM WPŁYWIE ROZBŁYSKÓW SŁONECZNYCH

Abstract

Solar variations modify a layer of the Earth's upper atmosphere known as the ionosphere. This is of particular concern for the aviation sector because of the way its communications and navigation systems can be affected. At the same time, one of the most complex atmospheric effects is the response of ionospheric regions to geomagnetic storms. The ionospheric response during the same storm can vary in time in different locations, which can introduce significant errors/displacement (meters) in single-frequency relative GNSS positioning (DGNSS technology). The residual effect can be somewhat mitigated by using dual- or multi-frequency GNSS, but dual frequency is not a guarantee against degradation of relative observations results, especially during significant geomagnetic storms. In this regard, PPP absolute positioning technology can be effective. However, another atmospheric effect – ionospheric scintillation can have a significant impact on the accuracy of both GNSS positioning approaches. The main goal of this study was to analyze the effect of second-order ionospheric delay during geomagnetic storms and ionospheric scintillations on GNSS positioning using the PPP method. GNSS data corrected

Streszczenie

Wahania aktywności Słońca modyfikują górną warstwę atmosfery Ziemi, zwaną jonosferą. Jest to szczególnie niepokojące dla sektora lotnictwa ze względu na wpływ, jaki może to mieć na jego systemy łączności i nawigacji. Jednocześnie jednym z najbardziej złożonych efektów atmosferycznych jest reakcja obszarów jonosfery na burze geomagnetyczne. Reakcja jonosfery podczas tej samej burzy może zmieniać się w czasie w różnych lokalizacjach, co może powodować znaczne błędy/przemieszczenia (rzędu kilku metrów) we względnym pozycjonowaniu GNSS przy jednej częstotliwości (technologia DGNSS). Efekt resztkowy można w pewnym stopniu złagodzić, stosując dwu- lub wieloczęstotliwościowy GNSS, jednak podwójna częstotliwość nie gwarantuje zapobiegania degradacji wyników względnych obserwacji, szczególnie podczas silnych burz geomagnetycznych. Pod tym względem skuteczna może być technologia pozycjonowania absolutnego PPP. Jednak inny efekt atmosferyczny – scyntylacja jonosferyczna może mieć znaczący wpływ na dokładność obu podejść do pozycjonowania GNSS. Głównym celem pracy była analiza wpływu opóźnienia jonosferycznego drugiego rzędu podczas burz geomagnetycznych i scyntylacji jonosferycznych na pozycjonowanie

Artykuł wpłynął do redakcji: 10.05.2023 / Zatwierdzono do publikacji: 24.06.2023

and uncorrected for higher-order ionospheric delay, respectively, were processed by the static PPP-AR method using the PRIDE-PPPAR ver.2.2.6 software for the selected periods of geomagnetic storms. From the analysis of the influence of second-order ionospheric errors, it follows that their values can reach almost 4 cm for first-frequency signals under different states of ionospheric disturbances for the GPS constellation and almost an order of magnitude less for the GNSS quadroconstellation. The appearance of stronger geomagnetic storms increases the second-order ionospheric errors by several millimeters.

Keywords: GNSS, precise point positioning (PPP), geomagnetic storm effects, ionosphere, second-order ionospheric term

GNSS metodą PPP. Dane GNSS skorygowane i nieskorygowane pod kątem opóźnienia jonosferycznego wyższego rzędu przetworzono statyczną metodą PPP-AR z wykorzystaniem oprogramowania PRIDE-PPPAR wersja 2.2.6 dla wybranych okresów burz geomagnetycznych. Z analizy wpływu błędów jonosferycznych drugiego rzędu wynika, że ich wartości mogą sięgać prawie 4 cm dla sygnałów pierwszej częstotliwości w różnych stanach zaburzeń jonosferycznych dla konstelacji GPS i prawie o rząd wielkości mniej dla kwadrokonstelacji GNSS. Pojawienie się silniejszych burz geomagnetycznych zwiększa błędy jonosferyczne drugiego rzędu o kilka milimetrów.

Słowa kluczowe: GNSS, precyzyjne pozycjonowanie punktów (PPP), burze geomagnetyczne, jonosfera, opóźnienia jonosferyczne drugiego rzędu

1. INTRODUCTION

Today, the requirements for stability of operation and accuracy of global navigation systems (GNSS) are constantly increasing. With the improvement of GNSS technologies, the accuracy and stability of data from these systems increasingly depends on the signal propagation environment, mainly on the state of the ionosphere. The Earth's ionosphere is a heterogeneous plasma containing a high concentration of ionized gas molecules. It is quite heterogeneous, which is why the density of ionized gas varies depending on the place of observation and time. Radio signals in the satellite-to-Earth path can be significantly affected by the disturbed ionosphere. This can lead to severe jitter in the amplitude and phase of the radio signals used in GNSS systems and affect the performance of these systems.

The analysis of the relationship between space weather and aviation is a relatively new and intensively developing research topic[1, 2, 3, 4, 5]. Since early 2002, the International Civil Aviation Organization (ICAO) has been assessing the need to provide space weather information for international air navigation during solar flares, and now ICAO provides real-time and worldwide space weather updates to aviation to help

1 G. Hubert, S. Aubry, *Study of the impact of past extreme solar events on the modern air traffic*, "Space Weather" 2021, vol. 19.

2 C. Marque, K.L. Klein, C. Monstein, H. Opgenoorth, A. Pulkkinen, S. Buchert, S. Krucker, R. van Hoof, P. Thulesen, *Solar radio emission as a disturbance of aeronautical radionavigation*, "J. Space Weather Space Clim" 2018, vol. 65.

3 H. Haukka, A.M. Harri, K. Kauristie, J. Andries, M. Gibbs, P. Beck, J. Berdermann, L. Perrone, B. van den Oord, D. Berghmans, N. Bergeot, E. De Donder, M. Latocha, M. Dierckxsens, H. Haralambous, I.M. Stanislawska, V. Wilken, V. Romano, M. Kriegel, K. Österberg, *PECASUS - ICAO Designated Space Weather Service Network for Aviation*, EGU General Assembly 2020, Online, 4–8 May 2020, EGU2020-7650.

4 K. Kauristie, J. Andries, P. Beck, J. Berdermann, D. Berghmans, C. Cesaroni, E. De Donder, J. de Patoul, M. Dierckxsens, E. Doornbos et al., *Space Weather Services for Civil Aviation – Challenges and Solutions*, "Remote Sens" 2021, vol. 13.

5 G. Grunwald, A. Ciećko, T. Kozakiewicz, K. Krasuski, *Analysis of GPS/EGNOS Positioning Quality Using Different Ionospheric Models in UAV Navigation*, „Sensors" 2023, vol. 23(3).

 DOI: 10.55676/asi.v3i1.54

ensure flight safety[6]. Today, the growing concern about space weather in aviation is mainly related to safety concerns, as safety is indeed at its core. However, the real impact of space weather on aviation may go far beyond safety issues. We still do not know which aspects of aviation will be affected by space weather and how space weather will affect certain aspects of aviation.

Changes in the ionosphere are amplified during periods of increased solar activity, which occur at the beginning and peak of the next solar cycle, and GNSS users experience two distinct effects:

The first effect – directly increased ionospheric activity – can introduce large errors/displacements (up to 15 meters) in single-frequency DGNSS due to the inability of the differential process to minimize the effect of the ionospheric delay between the reference station and the user. When using GNSS technologies based on two or more frequencies, the influence of the ionosphere can be eliminated almost completely, although, depending on the choice of differential approaches (double-differenced observation) or absolute positioning (undifferenced GNSS processing), this procedure has its own peculiarities in these two approaches. This becomes especially noticeable in the conditions of geomagnetic storms.

The second effect is scintillation, which is a rapid fluctuation in the amplitude and phase of GNSS signals as they pass through the ionosphere. These fluctuations can have a significant impact on the accuracy of GNSS positioning and even cause complete loss of satellite signals. Flicker occurs mainly in the evening along the geomagnetic equator. This leads to fluctuations in the amplitude and phase of the carrier phase signal, additional noise, or even loss of communication with the satellite. This can result in a reduction in the number of usable GNSS satellites. Scintillation effects are typically observed six hours after sunset, but cannot be predicted.

Increased ionospheric activity is correlated with the following factors:

- sunspot activity – increased ionospheric activity associated with the 11-year solar cycle;
- solar and magnetic storms – cause increased ionospheric activity;
- geographic location – highest activity along the geomagnetic equator and in polar regions;
- seasonal variations – increased activity on the vernal and autumnal equinoxes;
- daily variations – maximum effects are usually observed one hour after local sunset to midnight.

The current solar cycle 25 began in December 2019 and will last until approximately 2030 with an expected peak in July 2025. This cycle is already showing signs of exceeding predicted levels with significantly elevated levels of solar activity that are growing faster than expected. Thus, Solar flares (SFs), coronal mass ejections (CMEs) and solar energetic particles (SEPs) are typical space weather events.

[6] International Civil Aviation Organization, Annex 3 to the Convention on International Civil Aviation--Meteorological Service for International Air Navigation; Technical report; ICAO, Canada, Montréal 2018.

A large number of works have been devoted to the study of the impact of various space weather factors (geomagnetic storms, solar flares, etc.) on the stability and accuracy of GNSS positioning[7, 8, 9]. Over the past ten years, numerous and extensive studies have focused on the morphology and mechanisms of ionospheric storms based on the TEC (Total Electron Content) of the ionosphere derived from GNSS data and revealed some features of global and local storm evolution.

It should be noted that GNSS technologies have been significantly updated during this time (multi-frequency multi-GNSS, high-precision products, PPP with ambiguity resolution, etc.) and this, accordingly, affects the quality of applications, including ionospheric research.

A significant number of scientific GNSS applications require high accuracy of positioning and time transmission. Differential GNSS (relative positioning method), based on a network of observation stations, is currently the best tool for achieving such accuracy, as it usually eliminates most of the errors that affect satellite signals. However, for most scientific GNSS applications of the highest accuracy, this network approach leads to significant correlations and very often eliminates local environmental features. Precision point positioning (PPP) is an absolute positioning method that originated as an alternative to the relative positioning method. This method has been widely used in many applications in recent years, especially with the widespread introduction of precision products from various scientific organizations and institutions. An important source of error in PPP is the residual higher-order (second- and third-order) ionospheric error[10] (Elsobeiey and El-Rabbany, 2011) after the first-order ionospheric error has been removed by dual-frequency combinations of observations.

The goal of this paper is to analyze the effect of second-order ionospheric delay during geomagnetic storms and ionospheric scintillations on GNSS positioning using the PPP method. Three experiments were conducted to investigate the relationship between the effect of second-order ionospheric delay on the calculated coordinates during geomagnetic storms.

2. MATERIALS AND METHODS

2.1. Datasets and Processing Strategies

The observation data used in our study were collected from GNSS stations of the EPN (EUREF Permanent Network) network located in the eastern half of Poland and the

7 S. Bassiri, G.A. Hajj, *Higher-order ionospheric effects on the global positioning system observables and means of modeling them*, "Manuscr. Geod." 1993, vol. 18, 280.

8 W. Zhang, D.H. Zhang, Z. Xiao, *The influence of geomagnetic storms on the estimation of GPS instrumental biases*, "Ann Geophys" 2009, vol. 27, p. 1613–1623.

9 M. Garcia-Fernandez, S. Desai, M. Butala, A. Komjathy, *Evaluation of different approaches to modeling the second-order ionospheric delay on GPS measurements*, "J. Geophys. Res. Space Phys." 2011, vol. 118, p. 7864–7873.

10 M. Elsobeiey, A. El-Rabbany, *Impact of second-order ionospheric delay on GPS precise point positioning*, "J. Appl. Geophys." 2011, vol. 5, p. 37–45.

 DOI: 10.55676/asi.v3i1.54

western part of Ukraine (see Figure 1). Since there were only 7 stations from this network in this region: JOZE00POL (Jozefoslaw, POL), USDL00POL (Ustrzyki Dolne, POL), KRAW00POL (Krakow, POL), BPDL00POL (Biala Podlaska, POL), SULP00UKR (Lviv, UKR), RVNE00UKR (Rivne, UKR), FRA200UKR (Ivano-Frankivsk, UKR), several stations from the national reference GNSS networks VRSNET (Poland) were taken to provide sufficient latitude and longitude coverage: DLIN (Deblin), and ZAKPOS (Ukraine): KOEL (Kovel). It should be noted that the main station at which the entire range of studies was carried out was the GNSS station DLIN (Deblin, PL). At the other stations, only control studies were conducted to verify the results obtained.

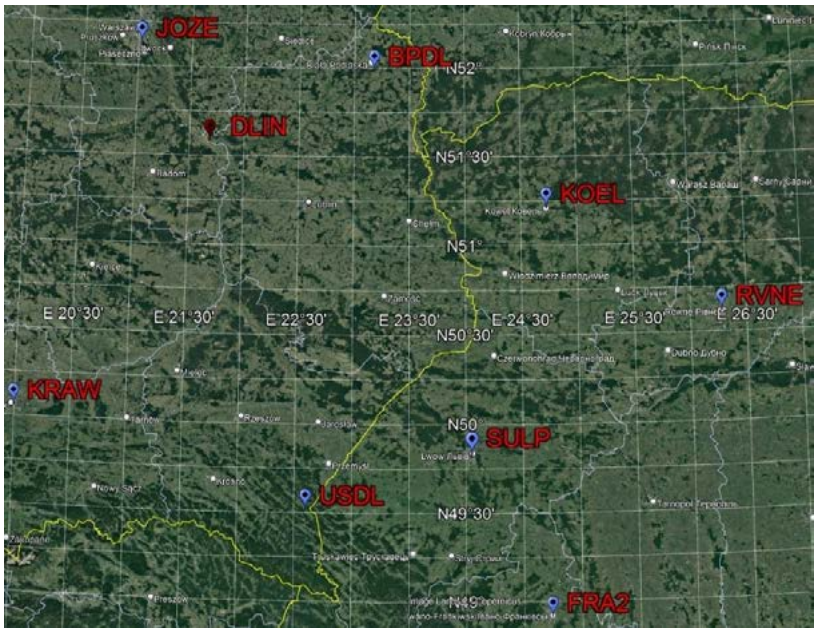

Figure 1. The distribution of GNSS stations used for analysis
Source: own study.

GNSS datasets from the first half of 2023 were generated on the selected dates to investigate the influence of second-order effects under different ionospheric conditions. Table 1 shows the values of increased geomagnetic parameters from February to June 2023 according to various international centers GODDARD Space Flight Center[11], World Data Center in Kyoto[12], SpaceWeatherLive[13], GFZ German Research Center for Geosciences[14], SPACE WEATHER PREDICTION CENTER[15]. In January and

11 https://omniweb.gsfc.nasa.gov [access: 25.08.2023].
12 http://wdc.kugi.kyoto-u.ac.jp/wdc/Sec3.html [access: 25.08.2023].
13 https://www.spaceweatherlive.com/en/solar-activity.html [access: 25.08.2023].
14 https://www.gfz-potsdam.de/en/section/geomagnetism/data-products-services/geomagnetic-kp-index [access: 25.08.2023].
15 https://www.swpc.noaa.gov/products-and-data [access: 25.08.2023].

July, no extreme indicators were observed, although they were slightly higher than the background.

Table 1. Geomagnetic disturbances in the first half of 2023

Date	Substorm class	Kp Index	Ap Index	Solar flares	
02	11		3+	8	X1.1
	15	G1	5+	27	M2.0
	16	G1	5	23	M1.1
	17		3	6	X2.2
	26	G2	6-	24	C5.4
	27	G3	7-	91	C4.5
	28	G2	6-	26	M8.62
03	04		4	20	X2.07
	23	G3	7	55	B9.6
	24	G4	8	73	C2
	25		4-	14	C1.6
	29		2	18	X1.2
04	23	G4	8+	65	C2.2
	24	G4	8	72	C2.8
05	6	G2	6	29	C5.2
	20	G2	6-	32	M8.96
	21	G2	6-	26	M2.6
06	15	G1	5+	26	C9.6
	16	G2	6	32	M1.0

Source: own study based on: SpaceWeatherLive[16] for getting substorm class and solar flares values; GFZ German Research Center for Geosciences[17] for obtaining Kp and Ap index.

As can be seen from Table 1, the largest geomagnetic storm in this period of time was observed on March 24 and April 23–24, respectively (class G4), while the highest solar activity was observed on February 11, 17, and March 4 and April 10. This is confirmed by the data shown in Figure 2.

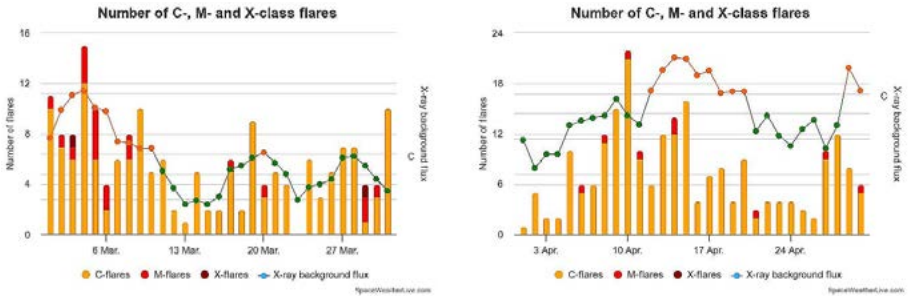

Figure 2. Solar activity (number and classes of solar flares) in March and April 2023

Source: SpaceWeather Live resource, https://www.spaceweatherlive.com/en/solar-activity/solar-cycle.html [access: 25.08.2023].

16 https://www.spaceweatherlive.com/en/solar-activity.html [access: 25.08.2023].

17 https://www.gfz-potsdam.de/en/section/geomagnetism/data-products-services/geomagnetic-kp-index [access: 25.08.2023].

 DOI: 10.55676/asi.v3i1.54

Based on the above data, it is impossible to predict the peaks of ionospheric activity on GNSS signals. It may be necessary to conduct an in-depth analysis of the impact of solar-magnetic coupling on a particular region of the Earth. This can be seen more clearly based on the behavior of the so-called Index-95, a value obtained from the analysis of data from a network of active reference stations. Thus, according to the ASG-EUPOS network[18], the highest ionospheric activity was observed on February 15, March 23–24, and April 23–24. It was somewhat lower on May 20–21 and June 15–16, 2023. Figure 3 shows the temporal change of the Index95 on the specified dates, where its anomalous values are clearly visible.

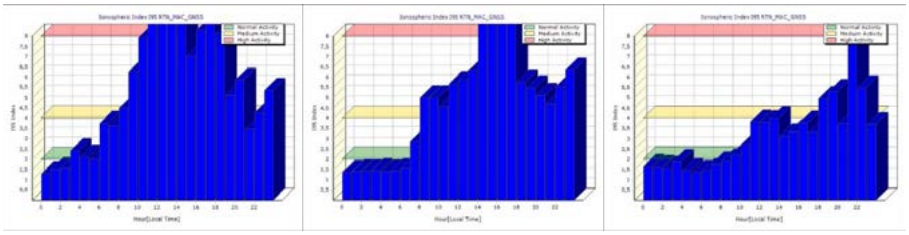

a) b) c)

Figure 3. Ionospheric activity (Index95) on February 15 (a), March 23 (b) and April 23 (c), 2023
Source: ASG-EUPOS website, https://system.asgeupos.pl/Iono/Ionosphere.aspx [access: 25.08.2023].

Figure 4a shows a graph of changes in the TEC parameter obtained from the GNSS data of the DLIN station in the GPS-TEC analysis software package for February 15, 2023. For comparison, a similar change on a calmer day – May 17, 2023 – is shown next to it (Figure 4b).

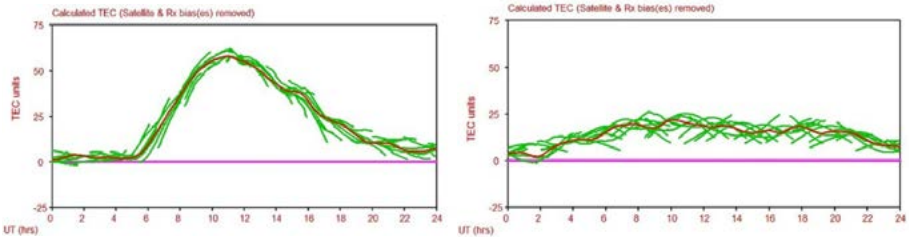

a) b)

Figure 4. Ionospheric activity (TEC) on February 15 (a) and May 17 (b), 2023
Source: own study.

[18] http://www.asgeupos.pl/ [access: 25.08.2023].

Next, we define the periods when ionospheric storms occurred as the "active period" (DOY[19] 45-48, DOY 82-84, DOY 109-114), and the period with low geomagnetic index and solar index as the "quiet period" (DOY 134-138) in 2023. It was for these periods that we processed the GNSS data. The „silent period" was considered to be, when the ionosphere is in its natural undisturbed state, and the processing results were considered to be control.

Table 2 summarizes the details of the PPP processing strategy. The processing itself was carried out in a Linux environment using the PRIDE PPP-AR software package[20]. The peculiarity of the processing was the double determination of the coordinates of the observation stations: first, it was carried out without taking into account the second-order ionosphere, and then with it. It should also be noted that the processing mode used was kinematic in the form of a fixed solution.

Table 2. Processing strategies of precise point positioning (PPP)

Item	Processing strategies
GNSS satellites	GPS, GLONASS, Galileo, BDS-2/3
File format	RINEX-3 support
Satellite product	Satellite orbit, Satellite clock, ERP, Quaternions, Code/phase bias (Precise products)
Tides (solid/ocean/pole)	Corrected
Observation	Ionosphere-free (IF) combination
Sampling rate	10 s
Elevation mask	7°
Weight for observations	Elevation-dependent weighting scheme
Estimator	Kalman filter
Ionosphere	With and without second-order corrections
Tropospheric mapping function	VMF3
Tropospheric wet delay	Estimated as random-walk model
Tropospheric gradients	Estimated as random-walk model
Phase center offset and variation	IGS Convention
Phase windup effect	Corrected

Source: own study.

From the initial data obtained from the "active period" (calculated coordinates), it is possible to determine the coordinate difference by comparing the coordinates of the "silent period" (control coordinates) with the calculated coordinates. These differences were further used to analyze the influence of second-order ionospheric errors.

2.2. Methodology

When a GNSS signal propagates through the ionosphere, phase advance and code delay occur, and its trajectory is bent. If we take into account the fact that at inclination angles > 7–10°, the trajectory bending error is about three orders of magnitude smaller than the phase delay error, the total ionospheric delay error can

[19] DOY –Day Of Year.

[20] J. Geng, X. Chen, Y. Pan et al., *PRIDE PPP-AR: an open-source software for GPS PPP ambiguity resolution. GPS Solutions*, "GPS Solut." 2023, vol. 23: 91, 2019.

 DOI: 10.55676/asi.v3i1.54

be represented by the sum of the ionospheric delay values of the first, second and third orders[21]:

$$I = \frac{e^2}{8\pi^2 \cdot \varepsilon_0 \cdot m \cdot f^2} \int N_e ds + \frac{-\mu_0 \cdot e^3 \cdot B_0 \cdot cos\theta}{16\pi^3 \cdot \varepsilon_0 \cdot m^2 \cdot f^3} \int N_e ds + \frac{-e^2}{128\pi^4 \cdot \varepsilon_0^3 \cdot m^2 \cdot f^4} \int N_e ds \quad (1)$$

Where:

e = 1,60218 · 10^{-19} is the amount of charge carried by the electron;

f is the carrier frequency; ε_0 = 8,8542 · 10^{-12} is the vacuum dielectric coefficient;

m = 9,10939 · 10^{-31} is the electron mass;

B_0 is the geomagnetic field strength along the propagation path;

θ is the angle between the GNSS signal propagation direction and the geomagnetic field;

$\int N_e ds$ represents the path integral of electron N_e from satellite s to receiver r.

Traditionally, to correct the first-order ionospheric delay, ionospheric-free combinations (IF) are formed, leaving the second- and third-order terms uncorrected.

As can be seen from Equation (1), to account for the influence of the second-order ionosphere, the values of B_0, θ and integral $\int N_e ds$ must be known. As for the first two parameters, they can be determined based on a known magnetic field model and ephemeral information for a particular observation station. That is, the magnetic field vector B_0 for the ionospheric piercing point (IPP) can always be calculated from a model, for example, IGRF-12[22], and the angle θ can be calculated from the given satellite ephemeris files and station coordinates. The time-dependent electron density $N_e = N_e(\varphi, \lambda, h, t)$, after integration along the beam path between the satellite position P^s and receiver P_r, is assumed to be equal to the total electron content (STEC – Slant Total Electron Content):

$$STEC(P^s, P_r, t) = \int_{Ps}^{P_r} N_e(\varphi, \lambda, h, t) ds. \quad (2)$$

Thus, the second component of equation (1), which is associated with the second-order ionospheric correction, can be represented as a function of STEC and geomagnetic induction. In this study, the global model IGRF 12 was used to obtain the geomagnetic induction[23].

STEC can be calculated from dual-frequency GNSS observations[24]:

$$STEC = \frac{1}{40{,}3} \times \frac{f_1^2 \cdot f_2^2}{f_2^2 - f_1^2} \times [(P_1 - P_2) - c \cdot (DCB_r + DCB_s)] \quad (3)$$

---

21 F.K. Brunner, M. Gu, *An improved model for the dual frequency ionospheric correction of GPS observations*, "Manuscr. Geod." 1991, vol. 16, p. 205–214.

22 https://www.ncei.noaa.gov/products/international-geomagnetic-reference-field [access: 25.08.2023].

23 E. Thébault, C.C. Finlay, C.D. Beggan, P. Alken, J. Aubert, O. Barrois, E. Canet, *International geomagnetic reference field: The 12th generation*, "Earth, Planets and Space" 2015, vol. 67(1), p. 79.

24 M. Fritsche, R. Dietrich, C. Knöfel, A. Rülke, S. Vey, M. Rothacher, P. Steigenberger, *Impact of higher-order ionospheric terms on GPS estimates*, „Geophys. Res. Lett." 2005, vol. 32, p. L23311.

where DCB_s is the differential code shift in the satellite path, which can be obtained from the Center for Orbit Determination in Europe[25], DCB_r is the differential code shift in the receiver path, which can be determined based on the assumption that VTECs calculated from different satellites at a certain inclination angle are close to each other[26]. Then, the receiver's DCB_r can be estimated by minimizing the standard deviation of the VTECs. Another approach to estimating the DCB_r is based on using the vertical TEC value from the global ionospheric map (GIM) based on linearly constrained least squares methods[27]. The residual term ϵ is the unmodeled error. The conversion of STEC to VTEC is achieved by introducing an isotropic reflection function depending on the slope angle.

3. RESULTS AND DISCUSSION

Given that the second-order ionospheric delay is a function of the TEC and the geomagnetic field, three experiments were conducted to investigate the relationship between the effect of this delay on the calculated coordinates during geomagnetic storms and the reference coordinates of the observation station.

The first experiment consisted of comparing the projected values from the vertical TPP, which was obtained from the global ionospheric maps (GIM)[28] from CODE, the $STEC_{GIM}$ values and the calculated $STEC_{Calc}$, values obtained from GNSS data of the selected observation stations in the GPS-TEC analysis software package[29]. The comparison was based on the differences in coordinates (reference and calculated) for all selected GNSS stations. The calculated coordinates when using $STEC_{GIM}$ were determined by taking into account the second-order ionosphere directly from the PRIDE PPP-AR software package. Topocentric coordinates were obtained in a similar way, but with the replacement of $STEC_{Calc}$. The result was the differences in topocentric coordinates ΔN, ΔE, ΔU for all stations and selected observation periods. The trends in these differences were very similar for the selected stations. Table 3 shows the statistical indicators for the DLIN GNSS station.

[25] CODE – Center for Orbit Determination in Europe, http://ftp.aiub.unibe.ch/ [access: 25.08.2023].

[26] Y. Zhang, F. Wu, N. Kubo, A. Yasuda, *TEC measurement by single dual-frequency GPS receiver*, In Proceedings of the 2003 International Symposium on GPS/GNSS, Tokyo, Japan, 15–18 November 2003, pp. 351–358.

[27] M. Keshin, *A new algorithm for single receiver DCB estimation using IGS TEC maps*, "GPS Solut." 2012, vol. 16, pp. 283–292.

[28] M. Hernández-Pajares, J.M. Juan, J. Sanz, R. Orus, A. Garcia-Rigo, J. Feltens, A. Komjathy, S.C. Schaer, A. Krankowski, *The IGS VTEC maps: A reliable source of ionospheric information since 1998*, "Journal of Geodesy" 2009, vol. 83(3–4), p. 263–275.

[29] https://seemala.blogspot.com/search/label/GPS-TEC%20RINEX%20analysis [access: 25.08.2023].

 DOI: 10.55676/asi.v3i1.54

Table 3. Statistical results of checking the coordinate differences (with $STEC_{GIM}$ and $STEC_{Calc}$) for DLIN station, mm

Differences of topocentric coordinates	DOY 45-48			DOY 82-84			DOY 109-114		
	mean	max	min	mean	max	min	mean	max	min
ΔN	1,06	2,14	1,18	1,30	2,88	1,54	2,00	3,45	1,02
ΔE	1,14	3,01	-0,56	1,66	2,65	1,23	1,95	3,24	1,01
ΔU	2,01	3,22	1,10	2,46	3,18	0,84	2,78	3,25	1,14

Source: own study.

As can be seen from Table 3, the differences in topocentric coordinates (control and calculated) show that their maximum values with the replacement of $STEC_{GIM}$ with $STEC_{Calc}$ do not exceed 1–2 mm.

The second experiment concerned the study of the intensity of ionospheric inhomogeneities by calculating the rate of change of TEC – ϑ_{TEC}. For this purpose, the difference of TEC of adjacent epochs divided by the sampling interval was determined:

$$\vartheta_{TEC}(in\frac{TECU}{minute}) = \frac{STEC_{Calc}(t+\Delta t) - STEC_{Calc}(t)}{\Delta t} \quad (4)$$

In our studies, the sampling interval was 10 s (see Table 2). We chose 5-minute intervals for estimating ϑ_{TEC}, to obtain a sufficiently high temporal resolution without implying any specific geomagnetic phenomenon. Table 4 shows the maximum values of $\vartheta_{TEC}(\frac{TECU}{minute})$ for «quiet period» (DOY 134–138) and «active periods» (DOY 45–48, DOY 82–84, DOY 109–114) for the selected GNSS stations.

Table 4. Statistical results of estimating the velocity ϑ_{TEC}, $\frac{TECU}{minute}$

GNSS stations	DOY 134–138	DOY 45–48	DOY 82–84	DOY 109–114
JOZE	0,35	4,25	5,18	6,12
USDL	0,34	4,18	5,54	6,01
SULP	0,34	4,51	5,09	5,96
DLIN	0,46	5,62	6,00	6,24
BPDL	0,41	5,53	5,91	6,14
KRAW	0,50	5,81	5,98	5,99
KOEL	0,53	5,44	6,05	6,02
RVNE	0,49	4,98	5,88	6,00
FRA2	0,51	5,72	5,95	6,22

Source: own study.

Thus, using a statistical analysis of the 10-second sampling rate, the threshold of the velocity ϑ_{TEC} or calm geomagnetic conditions – the "quiet period" according to the data of GNSS stations of the Polish-Ukrainian border is determined as 0,45 TECU/min. This same velocity shows good consistency across stations during

the period of calm ionosphere and becomes noticeably variable during periods of geomagnetic storms.

The third experiment was focused on detecting the influence of the second-order ionosphere in the conditions of geomagnetic storms. It concerned only the GPS constellation and the GNSS quadroconstellation, respectively. The comparison was based on the differences in coordinates (control and calculated) for all selected GNSS stations. The calculated coordinates were determined taking into account the second-order ionosphere (with ion) and without it (no ion). The result was the differences of topocentric coordinates dN, dE, dU for all stations and selected observation periods. The trends in these differences were very similar for the selected stations. Figure 5 shows the changes in the differences in the coordinates of the DLIN GNSS station for DOY 046 when using only the GPS constellation. When comparing these differences for all three periods of geomagnetic storms, it turned out that they could reach up to 4 cm.

Similarly, Figure 6 shows the changes in the differences in the coordinates of the DLIN GNSS station for DOY 046 when using the GNSS quadroconstellation. When comparing these differences for all three periods of geomagnetic drills, it turned out that they can reach up to 0.5 cm.

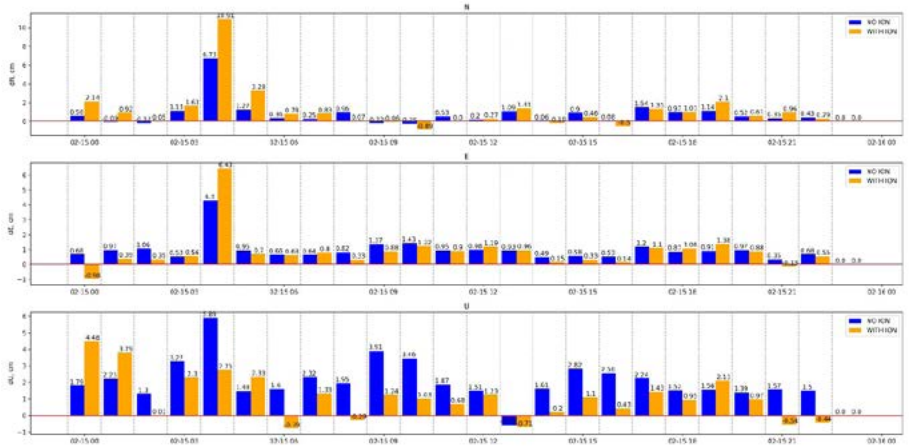

Figure 5. Changes in coordinate differences of the DLIN GNSS station for DOY 046 when using only GPS constellation

Source: own study.

 DOI: 10.55676/asi.v3i1.54

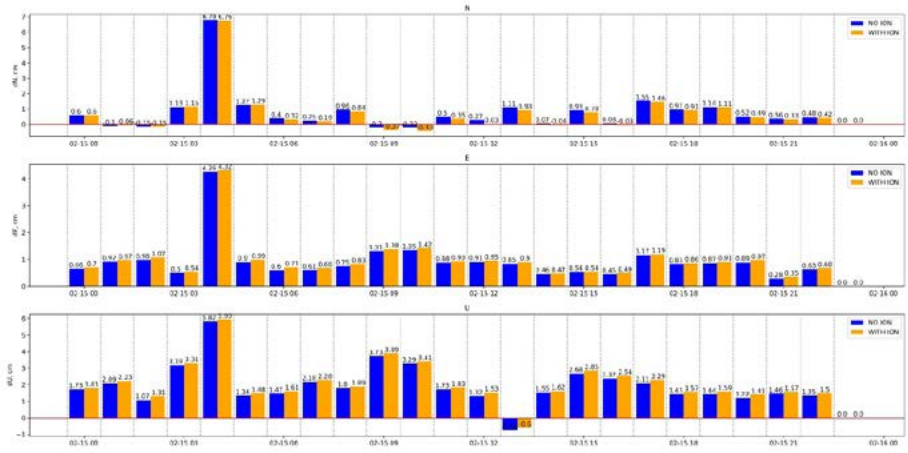

Figure 6. Changes in coordinate differences of the DLIN GNSS station for DOY 046 when using the GNSS quadroconstellation

Source: own study.

Thus, second-order ionospheric effects, if not properly accounted for, can affect the estimation of many parameters: tectonic motion rates, zenith tropospheric delays, horizontal tropospheric gradients, high-precision satellite orbit determination, differential coded offsets in the satellite-receiver path, etc.[30, 31, 32, 33]

4. CONCLUSIONS

In this study, a PPP-AR approach with quad-constellation (GPS, GLONASS, BDS and Galileo) is proposed to detect the effect of second-order ionospheric corrections on GNSS positioning during geomagnetic storms. GNSS data selected for the "active periods" for the first half of 2023 (DOY 45-48, DOY 82-84, DOY 109-114) were corrected and uncorrected for second-order ionospheric delay when processed by the static PPP-AR method using the PRIDE-PPPAR ver.2.2.6 software.

30 T. Hadas, A. Krypiak-Gregorczyk, M. Hernández-Pajares, *Impact and implementation of higher-order ionospheric effects on precise GNSS applications*, "J. Geophys. Res. Solid Earth" 2017, vol. 122, pp. 9420–36.

31 L. Yankiv-Vitkovska, S. Savchuk, *Monitoring the Earth Ionosphere by Listening to GPS Satellites*, [in:] *Knowledge Discovery in Big Data from Astronomy and Earth Observation. AstroGeoInformatics. Book*, ed. Petr Škoda, Fathalrahman Adam, 2020, pp. 385–404.

32 Li. Hang, W. Zemin, C. Xiangbin, G. Jingxue, L. Lin, S. Bo, *The effect of the second-order ionospheric term on GPS positioning in Antarctica*, Arctic, Antarctic, and Alpine, "Research" 2020, vol. 52(1), pp. 210–221.

33 F. Zus, Z. Deng, J. Wickert, *The impact of higher-order ionospheric effects on estimated tropospheric parameters in Precise Point Positioning*, "Radio Sci." 2017, vol. 52, pp. 963–971.

Main conclusions:

1. To take into account the influence of the second-order ionosphere, the value of the magnetic field vector B_0 for the point of penetration into the ionosphere must be known (we used the IGRF-12 model for this purpose, the angle between the direction of propagation of the GNSS signal and the geomagnetic field θ (we used satellite ephemeris files and the coordinates of the observation station) and the first-order ionospheric delay STEC. The PRIDE-PPPAR program uses the projected $STEC_{GIM}$ from the vertical TEC, which was obtained from the global ionospheric maps (GIMs) from CODE. We also used the calculated values of $STEC_{Calc}$, obtained from GNSS data of selected observation stations in the GPS-TEC analysis software package. The comparative analysis showed that the calculated $STEC_{Calc}$ values are slightly more accurate than the $STEC_{GIM}$, values modeled by GIM, but for the second order of the ionosphere this turned out to be insignificant.
2. Since the observation stations were selected at almost the same local time, the same parameter from different stations shows good temporal consistency (when outliers are eliminated). This made it possible to focus on a more detailed analysis of only one station. We only note that when the TEC changes > 6 TECU/min, the correlation of the same parameter from different stations decreases. However, the correlation improves significantly when the data is averaged daily.
3. From the analysis of the influence of the second-order ionosphere, it follows that its non-consideration can reach an error in coordinates of up to 4 cm for the first-frequency signals for the GPS constellation and almost an order of magnitude less for the GNSS quadroconstellation under different states of ionospheric disturbances. The emergence of stronger geomagnetic storms increases the second-order ionospheric errors by several millimeters.

Acknowledgments: The authors would like to thank EUREF Permanent Network (EPN) for providing the regional GNSS data and Center for Orbit Determination in Europe (CODE) for providing DCB products and the Global Ionospheric Map (GIM) as a reference ionosphere background. We thank the GNSS Research Center, Wuhan University for releasing the package PRIDE PPP-AR and Dr. Gopi Krishna Seemala from Indian Institute of Geomagnetism for the development of a computer program GPS-TEC analysis for calculation TEC from the GNSS observation.

BIBLIOGRAPHY

Bassiri S., Hajj G.A., *Higher-order ionospheric effects on the global positioning system observables and means of modeling them*, "Manuscr. Geod." 1993, vol. 18.

Brunner F.K., Gu M., *An improved model for the dual frequency ionospheric correction of GPS observations*, "Manuscr. Geod." 1991, vol. 16, https://doi.org/10.1134/S0016793207020120.

Elmas Z.G., Aquino M., Marques H.A., *Higher order ionospheric effects in GNSS positioning in the European region*, "Ann. Geophys." 2011, vol. 29, http://doi.org/10.5194/angeo-29-1383-2011.

Elsobeiey M., El-Rabbany A., *Impact of second-order ionospheric delay on GPS precise point positioning*, "J. Appl. Geophys." 2011, vol. 5, http://doi.org/10.1515/jag.2011.004.

Fritsche M., Dietrich R., Knöfel C., Rülke A., Vey S., Rothacher M., Steigenberger P., *Impact of higher-order ionospheric terms on GPS estimates*, "Geophys. Res. Lett." 2005, vol. 32, https://doi.org/10.1029/2005GL024342.

Garcia-Fernandez M., Desai S., Butala M., Komjathy A., *Evaluation of different approaches to modeling the second-order ionospheric delay on GPS measurements*, "J. Geophys. Res. Space Phys.c" 2011, vol. 118, http://doi.org/10.1002/2013JA019356.

Geng J., Chen X., Pan Y. et al., *PRIDE PPP-AR: an open-source software for GPS PPP ambiguity resolution*, "GPS Solutions" 2019, vol. 23, https://link.springer.com/article/10.1007/s10291-019-0888-1.

Grunwald G., Ciećko A., Kozakiewicz T., Krasuski K., *Analysis of GPS/EGNOS Positioning Quality Using Different Ionospheric Models in UAV Navigation*, "Sensors" 2023, vol. 23, https://doi.org/10.3390/s23031112.

Hadas T., Krypiak-Gregorczyk A., Hernández-Pajares M., *Impact and implementation of higher-order ionospheric effects on precise GNSS applications*, "J. Geophys. Res. Solid Earth" 2017, vol. 122, http://doi.org/10.1002/2017JB014750.

Hang Li, Zemin Wang, Xiangbin Cui, Jingxue Guo, Lin Li, Bo Sun, *The effect of the second-order ionospheric term on GPS positioning in Antarctica, Arctic, Antarctic, and Alpine*, "Research" 2020, vol. 52(1), https://doi.org/10.1080/15230430.2020.1742062.

Haukka H., Harri A.M., Kauristie K., Andries J., Gibbs M., Beck P., Berdermann J., Perrone L., van den Oord B., Berghmans D., Bergeot N., De Donder E., Latocha M., Dierckxsens M., Haralambous H., Stanislawska I.M., Wilken V., Romano V., Kriegel M., Österberg K., *PECASUS - ICAO Designated Space Weather Service Network for Aviation*, EGU General Assembly 2020, 4–8 May 2020, EGU2020-7650, https://doi.org/10.5194/egusphere-egu2020-7650.

Hernández-Pajares M., Juan J.M., Sanz J., Orus R., Garcia-Rigo A., Feltens J., Komjathy A., Schaer S.C., Krankowski A., *The IGS VTEC maps: A reliable source of ionospheric information since 1998*, "Journal of Geodesy" 2009, vol. 83 (3–4), https://doi.org/10.1007/s00190-008-0266-1.

Hoque M.M., Jakowski N., *Higher order ionospheric effects in precise GNSS positioning*, "J. Geod." 2007, vol. 81, https://doi.org/10.1007/s00190-006-0106-0.

Hubert G., Aubry S., *Study of the impact of past extreme solar events on the modern air traffic*, "Space Weather" 2021, vol. 19, e2020SW002665, https://doi.org/10.1029/2020SW002665.

ICAO, Annex 3 to the Convention on International Civil Aviation-Meteorological Service for International Air Navigation, Technical report, Canada, Montréal 2018.

Kauristie K., Andries J., Beck P., Berdermann J., Berghmans D., Cesaroni C., de Donder E., de Patoul J., Dierckxsens M., Doornbos E., et al., *Space Weather Services for Civil Aviation–Challenges and Solutions*, "Remote Sens." 2021, vol. 13, https://doi.org/10.3390/rs13183685.

Keshin M., *A new algorithm for single receiver DCB estimation using IGS TEC maps*, "GPS Solut." 2012, vol. 16, http://doi.org/10.1007/s10291-011-0230-z.

Liu Z., Li Y., Guo J., Li F., *Influence of higher-order ionospheric delay correction on GPS precise orbit determination and precise positioning*, "Geod. Geodyn." 2016, vol. 7, http://doi.org/10.1016/j.geog.2016.06.005.

Marque C., Klein K.L., Monstein C., Opgenoorth H., Pulkkinen A., Buchert S., Krucker S., van Hoof R., Thulesen P., *Solar radio emission as a disturbance of aeronautical radionavigation*, "J. Space Weather Space Clim." 2018, vol. 65, http://doi.org/10.1051/swsc/2018029.

Thébault E., Finlay C.C., Beggan C.D., Alken P., Aubert J., Barrois O., Canet E., *International geomagnetic reference field: The 12th generation*, "Earth, Planets and Space" 2015, vol. 67(1), https://doi.org/10.1186/s40623-015-0228-9.

Yankiv-Vitkovska L., Savchuk S., *Monitoring the Earth Ionosphere by Listening to GPS Satellites. In: Knowledge Discovery in Big Data from Astronomy and Earth Observation*, AstroGeoInformatics. Book, ed. P. Škoda, A. Fathalrahman, 2020, https://doi.org/10.1016/C2018-0-02187-8.

Zhang W., Zhang D.H., Xiao Z., *The influence of geomagnetic storms on the estimation of GPS instrumental biases*, "Ann Geophys" 2009, vol. 27, https://doi.org/10.5194/angeo-27-1613-2009.

Zhang Y., Wu F., Kubo N., Yasuda A., *TEC measurement by single dual-frequency GPS receiver*, Proceedings of the 2003 International Symposium on GPS/GNSS, Tokyo, Japan, 15–18 November 2003.

Zus F., Deng Z., Wickert J., *The impact of higher-order ionospheric effects on estimated tropospheric parameters in Precise Point Positioning*, "Radio Sci." 2017, vol. 52.

Internet resources

GPS-TEC RINEX analysis website, https://seemala.blogspot.com/search/label/GPS-TEC%20RINEX%20analysis.

Precise products, ftp://igs.gnsswhu.cn/pub/whu/phasebias/.

 DOI: 10.55676/asi.v3i1.54